

# Nanomaterials for Solar Energy Conversion: Dye-Sensitized Solar Cells Based on Ruthenium(II) *tris*-Heteroleptic Compounds or Natural Dyes

Juliana dos Santos de Souza, Leilane Oliveira Martins de Andrade,  
Andressa Vidal Müller and André Sarto Polo

## 1 Aims and Scope

Dye-sensitized solar cells, DSSCs, gained much attention since it is a simple and cheap device capable of converting the sunlight into electricity through a regenerative photoelectrochemical process. DSSCs overall efficiency attained up to 14% and it is estimated to last around 20 years. Besides the economic advantages, these devices can be transparent, which allows their use for distinct architectonic purposes such as facades of buildings. DSSCs are based on a nanocrystalline mesoporous semiconductor films sensitized by dyes, which are responsible for light harvesting and electron transfer, these processes start the energy conversion and are directly responsible for its overall efficiency.

This paper aims to review a specific class of synthetic dye, the *tris*-heteroleptic ruthenium sensitizers, which have been attracting much attention on the last years due to the possibility of tune their spectroscopic and electrochemical properties as well as to improve the stability of the device. The recent advances on the use of natural dyes as semiconductor sensitizers, from 2003 to 2016, are also reviewed.

## 2 Introduction

The use of fossil fuel based technologies is the major responsible for the continuous increase in the pollution and in the concentration of greenhouse gases. Renewable sources must have higher contribution on the energetic matrix in providing more energy available for the humanity in a short period, having low environmental

---

J.d.S. de Souza · L.O.M. de Andrade · A.V. Müller · A.S. Polo (✉)  
Centro de Ciências Naturais e Humanas, Universidade Federal do ABC,  
Av. dos Estados - 5001, Santo André - SP 09210-170, Brazil  
e-mail: andre.polo@ufabc.edu.br

impact [1, 2]. The interest on the conversion of environmentally friendly energy sources led to the development of several devices that took the advantage of the continuous evolution on several fields of research, which can result in new materials for already developed devices. For instance, the performance of direct methanol fuel cells, a well-known technology [3, 4] was improved due to the development of nanomaterials especially designed for the energy conversion process [5, 6] and their evolution allows the use of light to boost the process through a synergic arrangement [7–10].

The use of sunlight has been gaining much attention due to its abundance. For instance, it is possible to supply human energy needs up to year 2050 covering only 0.16% of the earth surface with 10% efficiency solar devices [1, 11]. There are several investigations on the conversion of sunlight in substances with more chemical energy than the reactants in a process that mimics the photosynthesis, this approach is known as artificial photosynthesis [12]. Most recently, the investigation on this research field is being called solar fuels and several papers were published describing photochemical approaches to produce high energy content substances, or fuels, from simple reactants such as water or  $\text{CO}_2$  [13–19].

Great interest is dedicated to an especially attractive device, the dye-sensitized solar cells, DSSC, since they are capable of converting the sunlight into electricity based on photoelectrochemical principles. The materials employed for the construction of these new solar cells are common and cheap and the procedures do not require controlled environment, thus clean rooms or any other sophisticated control can be avoided, consequently a very low production cost is estimated (less than 1 € per  $W_{\text{peak}}$ ) [20]. The use of new nanomaterials allows interesting features of these devices, such as transparency, possibility to have distinct colors, among others. These characteristics are very interesting for new applications of solar cells, since it can substitute glass windows and promote the co-generation of energy, or for any other architecture design.

Albeit the possible use of sensitization effect for solar energy conversion is known for a long time [21], the breakthrough of these solar cells was in 1991 when B. O'Regan and M. Grätzel published the use of nanocrystalline and mesoporous  $\text{TiO}_2$  film [22]. This film enhanced the light absorption due to its sponge-like characteristic which increases the surface area. The nanocrystallinity plays an important role on the electron injection and transport in these devices [23].

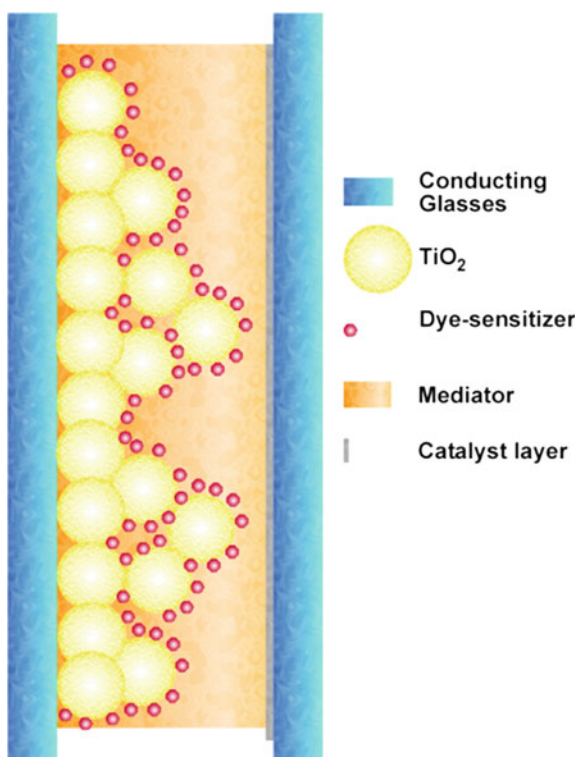
Since the paper of 1991, this field has been growing very fast and all the aspects of these solar cells are investigated [24–27]. In this review, the focus is on the development of *tris*-heteroleptic ruthenium (II) dyes as well as the use of natural extracts as a source of sensitizers. The absorption spectra and photoelectrochemical parameters published for these compounds since 2003 will be reviewed and discussed.

## 2.1 Dye-Sensitized Solar Cells—Principles and Operation

Dye-sensitized solar cells are prepared in a sandwich arrangement and are comprised by two electrodes, the photoanode and the counter electrode, Fig. 1. The photoanode is a conducting glass covered by a mesoporous and nanocrystalline  $\text{TiO}_2$  film, sensitized by the dye-sensitizers. The counter electrode is a conducting glass covered by a thin film of catalyst, such as platinum or graphite. Between these electrodes is placed a mediator layer, usually a solution of  $\text{I}_3^-/\text{I}^-$  in nitriles.

In order to promote the energy conversion, the sunlight is harvested by the dye-sensitizers leading to an excited state capable of inject an electron into the semiconductor conducting band. The oxidized dye is immediately regenerated by the mediator and the injected electron percolates through the semiconductor film, reaches the conducting glass, and flows by the external circuit to the counter electrode. The counter electrode is responsible for regenerating the oxidized specie of the mediator, reducing it by a catalyzed reaction using electrons from the external circuit. Since there is not a permanent chemical change for dye-sensitized solar cells, the estimated lifetime of these devices is 20 years [23].

**Fig. 1** Schematic arrangement of a dye-sensitized solar cell



## 2.2 Performance Experiments

Dye-sensitized solar cells are evaluated by several experimental approaches. For instance, the recombination processes or electron injection dynamics are investigated by time-resolved experiments [27–35], information about electron transport and electrical characteristics of  $\text{TiO}_2$  film can be obtained by electrochemical impedance spectroscopy [36]. Among several experiments used in evaluation of DSSCs, two experiments play an important role for investigation of dye performance, the current–voltage curves and photocurrent action spectra. Due to their importance, they are detailed in the next sections.

## 3 Current–Voltage ( $I \times V$ ) Curves

Current–voltage curves allow the access to one of the most important information about the prepared solar cells, the overall efficiency,  $\eta$ . Other important parameters such as the short-circuit current density,  $J_{\text{SC}}$ , open-circuit potential,  $V_{\text{OC}}$ , and fill factor,  $ff$ , are also determined by this experiment. In most cases,  $I \times V$  curves determined experimentally for dye-sensitized solar cells are similar to the schematic one, Fig. 2.

Short-circuit current density,  $J_{\text{SC}}$ , and open-circuit potential,  $V_{\text{OC}}$ , are the values determined by the intersection of  $I \times V$  curve to the current density axis. The voltage at this axis is zero, the short-circuit condition, thus the current is named for this condition. Analogous idea is applied for the determination of open-circuit potential, since the current at voltage axis is zero, open-circuit condition.

The maximum power output of a DSSC,  $P_{\text{max}}$ , is the highest value obtained for the multiplication of current density and voltage for each point of the  $I \times V$  curve and can be graphically expressed as the area covered by the orange rectangle in

**Fig. 2** Schematic current–voltage curve

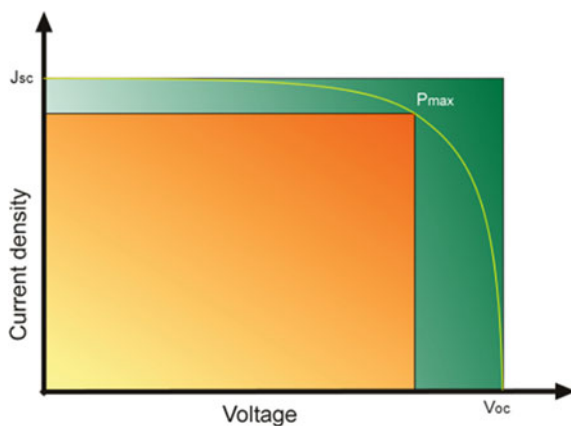


Fig. 2. On the other hand, the multiplication of  $V_{OC}$  by  $J_{SC}$  results in the maximum power output possible to be achieved for this DSSC and it can also be represented by the green rectangle of Fig. 2. The fill factor,  $ff$ , is named for the amount of the green rectangle which is filled by the orange one. Thus,  $ff$  express the electrical losses of DSSCs. Mathematically,  $ff$  can be determined by the ratio of  $P_{max}$  and the multiplication of  $J_{SC}$  by  $V_{OC}$ , Eq. 1.

$$ff = \frac{P_{max}(\text{mW cm}^{-2})}{J_{SC}(\text{mA cm}^{-2}) \cdot V_{OC}(V)} \quad (1)$$

Under simulated solar irradiation condition, (1 sun =  $P_{irr} = 100 \text{ mW cm}^{-2}$ ), the overall efficiency,  $\eta_{Cell}$ , can be determined by dividing  $P_{max}$  by the total incident light power,  $P_{irr}$ , Eq. 2, resulting in the percentage amount of solar light converted in electrical output.

$$\eta_{Cell}\% = \frac{P_{max}}{P_{irr}} \cdot 100\% \quad (2)$$

## 4 Photocurrent Action Spectra

Photocurrent action spectra exhibit the photoelectrochemical behavior of solar cells as a function of wavelength. For each wavelength, the incident photon-to-current conversion efficiency, IPCE, can be determined and the spectra are valuable to analyze the performance of new dyes prepared. IPCE values can be determined by a relationship that considers the energy and intensity of the incident light, the  $J_{SC}$  and Planck's constant, Eq. 3.

$$\text{IPCE}(\lambda) = \frac{J_{SC}}{P_{irr} \cdot e} \cdot \frac{hc}{\lambda} \quad (3)$$

- $J_{sc}$  Short-circuit photocurrent density ( $\text{A m}^{-2}$ );
- $h$  Planck's constant (J s);
- $c$  Speed of light ( $\text{m s}^{-1}$ );
- $\lambda$  Irradiation wavelength (nm);
- $P_{irr}$  Power of the incident light ( $\text{W m}^{-2}$ );
- $e$  Elementary charge (C).

For practical purposes, this equation can be simplified to Eq. 4.

$$\text{IPCE}\%(\lambda) = \left( 1239.8 \cdot \frac{J_{SC}(\text{mA cm}^{-2})}{P_{irr}(\text{mW cm}^{-2}) \cdot \lambda(\text{nm})} \right) \cdot 100\% \quad (4)$$

IPCE values are also related to some important parameters for DSSCs, such as light harvesting efficiency, LHE, electron injection quantum efficiency,  $\Phi_{\text{EI}}$ , and the efficiency of collecting electrons in the external circuit,  $\eta_{\text{EC}}$ , Eq. 5 [37]. The simple measurements, such as  $J_{\text{SC}}$  and  $P_{\text{irr}}$  allow the access to important information such as the electron injection quantum yield.

$$\text{IPCE}(\lambda) = \text{LHE} \Phi_{\text{EI}} \eta_{\text{EC}} \quad (5)$$

Photocurrent action spectra are valuable experiments to evaluate new dye-sensitizers since it is possible to directly associate the absorption response of the dye with the conversion efficiency. This is important information for designing new sensitizers.

## 4.1 Molecular Engineering

The design of new dye-sensitizers is based on joining in just one specie components capable of performing specific tasks. Using different ligands, it is possible to have excellent light harvesting, electron injection on semiconductor conducting band and fast regeneration by the mediator. A new molecule to be employed in DSSCs should fulfill some basic requirements such as having an intense absorption in the visible region, which corresponds to 44% of the incident sunlight on the earth's surface, having an anchoring group capable of promoting the chemical adsorption onto  $\text{TiO}_2$  surface, improving the electronic coupling between dye and semiconductor interface.

The first DSSC that exhibited  $\eta > 10\%$  employed *cis*-di(isothiocyanato)*bis*-(2,2'-bipyridyl-4,4'-dicarboxylic acid)ruthenium(II), N3, as dye-sensitizer [38]. After this dye, the complex *mer*-tri(isothiocyanato)(2,2',2''-terpyridyl-4,4',4''-tricarboxylic acid)ruthenium(II), black dye, was prepared and also successfully used as sensitizer [39], Fig. 3.

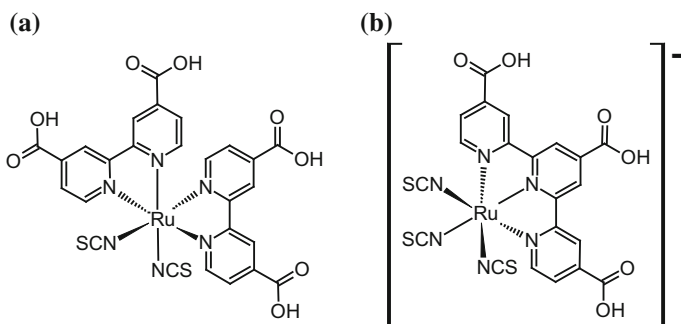


**Fig. 3** Structures of the N3 (a) and black dye (b) sensitizers

Due to the outstanding performance of N3 and black dye as dye-sensitizers, they can be used as models for molecular engineering of new dyes. Their chemical attachment onto  $\text{TiO}_2$  surface occur through the carboxylic acid groups of the 2,2'-bipyridine or of the 2,2',2''-terpyridine ligands. Particularly, the 4,4'-dicarboxylic acid-2,2'-bipyridine anchoring ligand is been widely employed among several other possible groups investigated and it has been considered the best one for ruthenium(II) sensitizers [40]. This ligand allows intimate electronic coupling between the dye excited state wave function and the semiconductor conducting band. Its lowest unoccupied orbital, LUMO, is the lowest one of the coordination compound and facilitates an efficient electronic transfer from excited dye molecules to titania nanocrystals [41].

Great influence on the absorption spectra and molar absorptivities of compounds, emission maxima and quantum yields, as well as excited state lifetimes, in addition to the redox properties was observed as a function of the degree of protonation of the carboxylic acids of the ligand. These changes are directly responsible for the increase on photovoltaic performance of solar cells sensitized by N719, Fig. 4, which is the di-deprotonated N3 specie [42]. As a natural consequence, the use of compounds having one or more deprotonated carboxylic groups in the  $\text{dcBH}_2$  has been increasing [32, 41, 43–48].

In the case of N3, consequently of N719, the presence of two  $\text{dcBH}_2$  ligands results in absorption spectra which overlaps the visible region of the incident sunlight. The absorption bands have high molar absorptivity ( $\epsilon \sim 10^4 \text{ L mol}^{-1} \text{ cm}^{-1}$ ), typical of metal-to-ligand charge transfer transitions,  $\text{MLCT}_{\text{d}\pi\text{Ru}-\pi^*\text{dcBH}_2}$ . The high molar absorptivity improves the light harvesting efficiency, allowing the absorption of almost all incident light in a few micrometers of optical length of the  $\text{TiO}_2$  film. Besides the bipyridine, the two isothiocyanate ligands in these complexes are valuable to promote the stabilization of the  $t_{2g}$  orbitals and result in a fine tuning of the energy levels of the complex.

## 5 Ruthenium *tris*-Heteroleptic Complexes

The knowledge acquired understanding the structure of the N3 dye can be used for the development of several other complexes by using the molecular engineering [49]. Among several classes of compounds developed, ruthenium *tris*-heteroleptic

**Fig. 4** Structure of N719

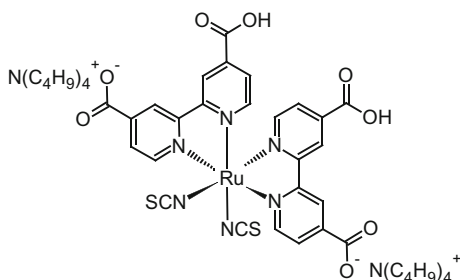
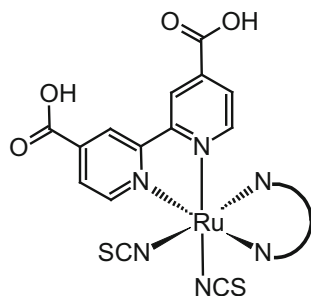


**Fig. 5** General structure of  $cis$ -[Ru(dcbH<sub>2</sub>)(L)(NCS)<sub>2</sub>] dyes



complexes have been gaining attention on the last years due to the possibility of modulate their properties, just changing one of the polypyridinic ligands. This approach is very interesting for the development of new sensitizers. A comprehensive review about these compounds was also published in 2016 [50].

There are several classes of ruthenium *tris*-heteroleptic compounds described by the general formula  $cis$ -[Ru(dcbH<sub>2</sub>)(L)(NCS)<sub>2</sub>], Fig. 5, since each new ligand L and its derivatives can be a new class. In this work, our focus will be on 2,2'-bipyridine derivatives and 1,10-phenanthroline derivatives, even that several other compounds of this general formula are known [34, 51–53].

### 5.1 2,2'-Bipyridine Derivative Ligands

The search for high-efficiency ruthenium(II) dyes is focused on the development of complexes having high molar absorptivity, mainly in visible and near infrared region [54, 55]. A good light harvesting yield and a reduction on the film thickness, which imply reduction of transport losses in the nanoporous environment, result in higher open-circuit potentials and more efficient devices [56, 57]. Another approach is the development of dye-sensitizers capable of improving the lifetime performance of a dye-sensitized solar cell.

The first *tris*-heteroleptic ruthenium compounds investigated as dye-sensitizers are based on 2,2'-bipyridine derivatives and it is possible to observe three different approaches, following the bipyridine substituent. These subclasses are the amphiphilic, donor antenna, and thiophene compounds.

## 6 Amphiphilic Compounds

In 2003, a thermally stable DSSC was disclosed employing the amphiphilic Z907 sensitizer. Using this dye it was possible to prepare stable devices under prolonged thermal stress at 80°. However, the molar extinction coefficient of this sensitizer is



somewhat lower than that of the standard N719 dye. Meanwhile, a compromise between efficiency and high temperature stability has been noted for the Z907 sensitizer [58]. Subsequently, the concept of developing a high molar extinction coefficient, amphiphilic ruthenium sensitizer, was followed by other groups, with a motivation to enhance device efficiency [34, 59–62]. The absorption properties as well as the performance parameters determined for ruthenium *tris*-heteroleptic complexes having amphiphilic derivatives of 2,2'-bipyridine are listed in Table 1.

The absorption spectra of amphiphilic compounds usually exhibit two MLCT bands in the visible region, typical of ruthenium *bis*-bipyridyl compounds. Molar absorptivity values listed on Table 1 are similar to those determined for the complexes N3 or N719. This behavior is expected since the aliphatic substituents do not have significant influence in the chromophoric properties of the complexes.

Amphiphilic ruthenium *tris*-heteroleptic dye-sensitizers exhibit lower photoelectrochemical performance than determined for N3. The highest efficiency achieved by this class of dyes is 8.6% [60]. The advantage of these compounds is their long-term stability. These amphiphilic heteroleptic sensitizers have the ground-state  $pK_a$  of 4,4'-dicarboxy-2,2'-bipyridine higher than determined for N3, enhancing the chemical adsorption of the complex onto the  $TiO_2$  surface [61, 70, 71]. The structure of amphiphilic ligands decreases the charge density on the sensitizer, resulting in less electrostatic repulsion and higher amount of dye adsorbed. The hydrophobic substituent of 2,2'-bipyridine does not allow the presence of water molecules close to  $TiO_2$  surface, improving the stabilization of solar cells toward water-induced desorption of the dye. The redox potentials of these complexes are shifted toward a more positive electrochemical potential in comparison to the N3 sensitizer, increasing the reversibility of the ruthenium III/II couple, leading to higher electrochemical stability [61, 70, 71].

## 7 Donor Antenna Compounds

Complexes prepared with donor antenna substituents of 2,2'-bipyridine are an approach to improve the light absorption at the same time that the hydrophobic character is enhanced. The use of aromatic substituents can have this function since the aromaticity increases the light absorption and the existence of the hydrophobic chain allows the protection to dye desorption caused by water. The spectral and photoelectrochemical parameters of this class of dyes are listed in Table 2.

In most cases, it is observed higher molar absorptivities values in comparison to amphiphilic compounds or N3 or N719 dyes which can be ascribed to an extended  $\pi$ -cloud delocalized in the substituent. The higher light harvesting efficiency results directly in higher IPCE values as well as overall efficiency of the solar cell, Table 2.

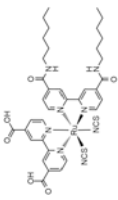
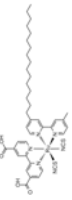
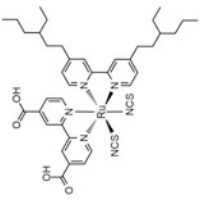
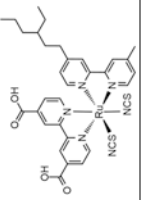
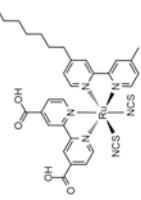
There are a few investigations on the use of  $\pi$ -excessive heteroaromatic rings as end groups in substituted bpy ligands [43, 44, 72]. The use of conjugated  $\pi$ -excessive heteroaromatic rings as end substituents donors directs the electron

**Table 1** Absorption properties and photoelectrochemical performance of ruthenium(II) *tris*-heteroleptic compounds having amphiphilic derivatives of 2,2'-bipyridine

Abbreviation	Structure	Absorption properties		Photoelectrochemical performance					References
		Solvent	$\lambda_{\text{MAX}}/\text{nm}$ ( $\epsilon_{\text{MAX}}/\text{cm}^{-1}$ )	$V_{\text{oc}}/\text{V}$	$J_{\text{sc}}/\text{mA cm}^{-2}$	IPCE <sub>MAX</sub> % ( $\lambda/\text{nm}$ )	$ff$	$\eta_{\text{cell}}$ %	
Z907		Ethanol	295 (4.24); 312 (3.01); 385 (1.09); 526 (1.16)	0.73	12.5	80 (540)	0.67	6.2	[58]
CS9		DMF	296 (4.17); 366 (1.03); 518 (0.7)	0.63	14.59	60 (540)	0.62	5.68	[59]
NMK-2 <sup>a</sup>		Ethanol	295 (4.54); 312 (3.35); 383 (1.13); 524 (1.16)	0.7	14.7	—	—	6.8	[60]
NMK-3 <sup>a</sup>		Ethanol	296 (4.26); 312 (3.2); 384 (1.01); 525 (1.11)	0.7	15.5	—	—	7.4	[60]
NMK-5 <sup>a</sup>		Ethanol	296 (4.21); 312 (3.02); 384 (1.08); 525 (1.15)	0.75	16.2	90	—	8.6	[60]
KC-8 <sup>a</sup>		DMF	297 (4.54); 309 (2.74); 370 (1.25); 522 (1.26)	0.673	17.13	86	0.72	8.3	[61]
A597		DMF	313 (5.2); 397 (1.6); 539 (1.8)	0.778	11.83	57 (540)	0.78	7.25	[63]

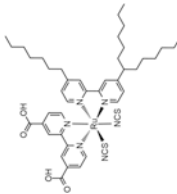
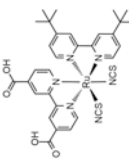
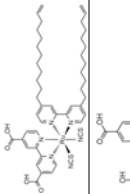
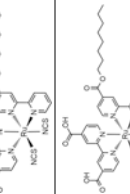
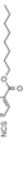
(continued)

Table 1 (continued)

Abbreviation	Structure	Absorption properties		Photoelectrochemical performance					References
		Solvent	$\lambda_{MAX}/nm$ ( $\epsilon_{MAX}/10^4 L mol^{-1} cm^{-1}$ )	$V_{oc}/V$	$J_{sc}/mA cm^{-2}$	IPCE <sub>MAX</sub> % ( $\lambda/nm$ )	$ff$	$\eta_{cell}$ %	
C4		Ethanol	312 (2.6); 391 (0.9); 535 (0.9)	0.71	15.5	75 (500)	0.66	7.3	[64]
C5		Ethanol	296 (3.65); 314 (2.53); 384 (1.0); 528 (1.01)	0.72	16.7	—	0.64	7.7	[64]
CS27		DMF	299 (4.78); 369 (1.25); 517 (1.13)	0.63	3.0	45	0.77	1.46	[65]
CS28		DMF	299 (4.48); 370 (1.20); 518 (1.08)	0.66	7.0	80	0.72	3.28	[65]
CS32		DMF	298 (4.50); 370 (1.17); 518 (1.05)	0.66	6.7	80	0.67	2.95	[65]

(continued)

Table 1 (continued)

Abbreviation	Structure	Absorption properties		Photoelectrochemical performance					References
		Solvent	$\lambda_{MAX}/nm$ ( $\epsilon_{MAX}/10^4\text{ L mol}^{-1}\text{ cm}^{-1}$ )	$V_{oc}/V$	$J_{sc}/\text{mA cm}^{-2}$	IPCE <sub>MAX</sub> % ( $\lambda/nm$ )	$ff$	$\eta_{cell}\%$	
CS43		DMF	299 (5.43); 369 (1.34); 518 (1.20)	0.69	6.1	70	0.69	2.91	[65]
K005		Ethanol	316 (2.68); 418 (0.95); 537 (0.94)	0.553	9.35	—	0.720	3.72	[66]
Ru-C		—	—	0.68	11.1	—	0.67	5.1	[67]
RuC9		Acetonitrile/ <i>t</i> -butanol (1:1 v/v)	215; 294; 379 (0.99); 521 (1.14)	0.673	14.10	—	0.711	6.92	[68]
S8		Ethanol	315; 395; 535	0.60	13.02	—	0.69	5.36	[69]

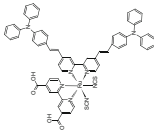
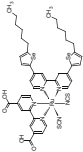
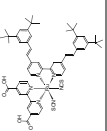
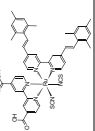
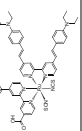
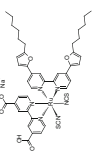
<sup>a</sup>These compounds were named after the initials of the first author of the reference cited

**Table 2** Absorption properties and photoelectrochemical performance of ruthenium(II) *tris*-heteroleptic compounds having donor antenna derivatives of 2,2'-bipyridine

Abbreviation	Structure	Absorption properties		Photoelectrochemical performance					References
		Solvent	$\lambda_{MAX}/nm$ ( $\epsilon_{MAX}/10^4\text{ L mol}^{-1}\text{ cm}^{-1}$ )	$V_{oc}/V$	$J_{sc}/\text{mA cm}^{-2}$	IPCE <sub>MAX</sub> % ( $\lambda/nm$ )	$\mathcal{F}$	$\eta_{cell}\%$	
LXJ1		DMF	309 (4.7), 353 (3.3), 549 (1.84)	0.715	16.50	83.7 (550)	0.745	8.80	[43]
IJ-1		Ethanol	218; 308 (5.0); 432 (4.3), 536 (1.9)	0.748	19.2	87	0.72	10.3	[56]
KW-2 <sup>a</sup>		DMF	310 (4.86); 373 (7.95); 550 (2.22)	0.685	3.42	—	0.42	0.99	[57]
KW-3 <sup>a</sup>		MeOH + 1 wt % KOH	307 (8.13); 429 (5.34); 524 (3.09)	0.735	4.03	—	0.46	1.37	[57]
KW-4 <sup>a</sup>		1:1 H <sub>2</sub> O; DMF + 1 wt% KOH	307 (3.88); 381 (1.28); 526 (1.13)	0.635	2.15	—	0.42	0.58	[57]

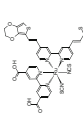
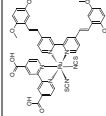
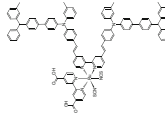
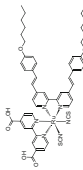
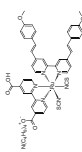
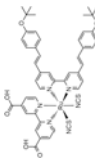
(continued)

Table 2 (continued)

Abbreviation	Structure	Absorption properties		Photoelectrochemical performance					References
		Solvent	$\lambda_{\text{MAX}}/\text{nm}$ ( $\epsilon_{\text{MAX}}/10^4 \text{ L mol}^{-1} \text{ cm}^{-1}$ )	$V_{\text{oc}}/ \text{V}$	$J_{\text{sc}}/ \text{mA cm}^{-2}$	IPCE <sub>MAX</sub> % ( $\lambda/\text{nm}$ )	$ff$	$\eta_{\text{cell}} \%$	
KW-5 <sup>a</sup>		1:1 H <sub>2</sub> O: DMF + 1 wt% KOH	304 (6.25); 423 (5.47); 544(2.27)	0.715	4.30	—	0.43	1.31	[57]
C105		DMF	309 (3.90); 353 (3.2); 420(1.84); 550 (1.84)	0.747	18.9	95 (520)	0.744	10.06	[72]
HRD-1		DMF	543 (1.93)	0.59	10.9	60	0.78	4.93	[70]
HRD-2		DMF	532 (1.61)	0.60	10.5	64	0.78	4.91	[70]
HRS-2		Ethanol	431 (5.93); 542 (2.81)	0.697	17.47	85 (552)	0.711	8.65	[71]
C102		DMF	305; 341; 407; 547 (1.68)	0.740	17.80	82 (550)	—	9.5	[44]

(continued)

Table 2 (continued)

Abbreviation	Structure	Absorption properties		Photoelectrochemical performance					References
		Solvent	$\lambda_{MAX}/nm$ ( $\epsilon_{MAX}/10^4\text{ L mol}^{-1}\text{ cm}^{-1}$ )	$V_{oc}/V$	$J_{sc}/\text{mA cm}^{-2}$	IPCE <sub>MAX</sub> % ( $\lambda/nm$ )	$ff$	$\eta_{cell}\%$	
AB-I <sup>a</sup>		Ethanol	314; 388; 538 (1.6)	0.663	19.1	87	0.72	9.1	[55]
N945		1:1 acetonitrile: <i>tert</i> -butanol	400 (3.4); 550 (1.9)	0.728	17.96	61	0.71	9.29	[73]
KCS-I <sup>a</sup>		DMF	310 (8.49); 440 (5.34); 540 (2.67)	0.757	9.6	—	0.35	3.4	[74]
K-19		DMF	310 (5.0); 350 (4.8); 410 (1.8); 545 (1.8)	0.718	13.2	—	0.745	7.1	[32]
K-73		DMF	310; 350; 410; 545	0.748	17.22	85 (540)	0.649	9.5	[32]
K77		DMF	310; 346; 546 (1.94)	0.737	17.5	90 (550)	0.696	9.0	[75]

(continued)

Table 2 (continued)

Abbreviation	Structure	Absorption properties		Photoelectrochemical performance					References
		Solvent	$\lambda_{\text{MAX}}/\text{nm}$ ( $\epsilon_{\text{MAX}}/10^4 \text{ L mol}^{-1} \text{ cm}^{-1}$ )	$V_{\text{oc}}/\text{V}$	$J_{\text{sc}}/\text{mA cm}^{-2}$	IPCE <sub>MAX</sub> % ( $\lambda/\text{nm}$ )	$ff$	$\eta_{\text{cell}}\%$	
Z-910		Acetonitrile	410 (1.7); 543 (1.69)	0.777	17.2	87 (520)	0.764	10.2	[33]
KC-5 <sup>a</sup>		DMF	313 (3.88); 392 (1.17); 537 (1.19)	0.695	15.8	75	0.66	7.01	[61]
KC-6 <sup>a</sup>		DMF	314 (3.36); 390 (1.11); 531 (1.12)	0.676	15.47	63	0.71	7.42	[61]
KC-7 <sup>a</sup>		DMF	312 (3.39); 393 (1.12); 533 (1.21)	0.676	16.11	79	0.7	7.62	[61]
MH06		DMF	390 (4.07); 541 (2.15)	0.642	15.07	70	0.692	6.70	[76]
MH11		DMF	414 (5.16); 547 (2.7)	0.671	19.70	90	0.664	8.78	[76]

<sup>a</sup>These compounds were named after the initials of the first author of the reference cited



injection in the excited state and enhances the oscillator strength resulting in significant increases in the short-circuit photocurrent [55].

The higher molar absorptivity in the visible region can be understood by the influence of the different delocalized  $\pi$ -systems integrated in the bipyridyl donor antenna ligands. The reason for the lower absorption of the standard N719 dye in this region is the absence of any these groups [57].

## 8 Thiophene Compounds

Ruthenium(II) sensitizers having 2,2'-bipyridine with thiophene substituents have higher molar absorptivity than observed for the previous classes of compounds. For instance, the compound KW-1 has  $\epsilon_{515} = 3.56 \text{ L mol}^{-1} \text{ cm}^{-1}$  [57], much higher than the ones determined for N3 or N719 dyes. As it is observed for the donor antenna class of compounds, the higher light harvesting efficiency results in higher IPCE values and consequently improves the overall performance of the solar cell, Table 3.

Ruthenium(II) thiophene compounds gained special attention after C101 dye has set a new DSSC efficiency record of 11.3–11.5% and became the first sensitizer to triumph over the well-known N3 dye [44]. In comparison to its analogues C102 or C105, in which the thiophene is replaced by furan, or selenophene, respectively, the molar absorptivity increases in the order of  $\text{Se} > \text{S} > \text{O}$ . This sequence it is consistent with the electropositivity trend and the size of the heteroatoms of five-member conjugated units. The LUMO energy sequence of the spectator ligand is  $\text{O} > \text{S} > \text{Se}$ , which explains this behavior [72].

Another important dye employing thiophene derivatives is CYC-B1, which exhibits a remarkably high light-harvesting capacity of up to  $2.12 \times 10^4 \text{ L mol}^{-1} \text{ cm}^{-1}$  [40]. After the development of the CYC-B1 dye, several ruthenium dyes were synthesized by incorporating thiophene derivatives into the ancillary ligand and DSSC cells based on these dyes exhibited excellent photovoltaic performances [45, 46, 77, 78].

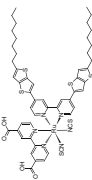
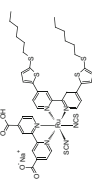
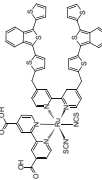
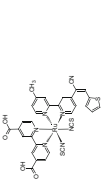
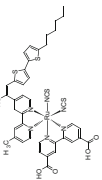
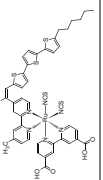
The extensive use of polythiophene is due to its similarity to a *cis*-polyacetylene chain bridged with sulfur atoms. The “bridging sulfur atoms” could effectively provide aromatic stability to the polyacetylene chain while preserving the desirable physical properties, such as high charge transport. The facile functionalization of thiophene groups also offers relatively efficient synthetic solutions to solubility, polarity, and energetic tuning. Furthermore, sulfur has greater radial extension in its bonding than the second-row elements, such as carbon. Therefore, thiophene is a more electron-rich moiety and incorporation of thiophene onto bipyridine ligands raises the energy levels of the metal center and the LUMO of the ligands [80]. As a consequence, the band resulting from charge transfer from the metal center to the anchoring ligand is redshifted, and upon illumination of the sample, the electrons on the metal center are transferred to the anchoring  $\text{dcBH}_2$  ligand, where electrons can move to the outer circuit through the  $\text{TiO}_2$  particles more efficiently [40].

**Table 3** Absorption properties and photoelectrochemical performance of ruthenium(II) *tris*-heteroleptic compounds having thiophene derivatives of 2,2'-bipyridine

Abbreviation	Structure	Absorption properties		Photoelectrochemical performance					References
		Solvent	$\lambda_{MAX}/nm$ ( $\epsilon_{MAX}/10^4 L mol^{-1} cm^{-1}$ )	$V_{oc}/V$	$J_{sc}/mA cm^{-2}$	IPCE <sub>MAX</sub> % ( $\lambda/nm$ )	$\mathcal{F}$	$\eta_{cell}$ %	
CYC-B1		DMF	312 (3.58); 400 (4.64); 553 (2.12)	0.65	23.92	77.5	0.55	8.54	[40]
CYC-B3		DMF	350; 400; 544 (1.57)	0.669	15.7	64.1 (520)	0.705	7.39	[77]
CYC- B7		DMF	345 (3.55), 412 (4.35), 551 (2.19)	0.788	17.4	76 (530)	0.654	8.96	[78]
CYC-B11		DMF	305(4.5), 388(5.40), 554 (2.42)	0.714	16.1	95 (580)	0.69	7.9	[45]
CYC-B13		DMF	295 (8.6); 397 (3.4); 547 (1.93)	0.728	10.26	90 (550)	0.68	5.1	[46]
C101		DMF	305; 341; 407; 547 (1.75)	0.746	5.42	89 (580)	0.833	11.3	[44]

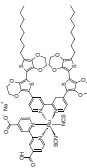
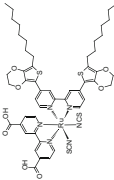
(continued)

Table 3 (continued)

Abbreviation	Structure	Absorption properties		Photoelectrochemical performance					References
		Solvent	$\lambda_{MAX}/nm$ ( $\epsilon_{MAX}/10^4\text{ L mol}^{-1}\text{ cm}^{-1}$ )	$V_{OC}/V$	$J_{SC}/\text{mA cm}^{-2}$	IPCE <sub>MAX</sub> % ( $\lambda/nm$ )	$ff$	$\eta_{cell}$ %	
C104		DMF	312 (5.4); 368 (4.5); 553 (2.05)	0.76	17.87	85 (580)	0.776	10.53	[62]
C106		DMF	310 (3.95); 348 (3.1); 550 (1.87)	0.749	18.28	90 (520–640)	0.772	10.57	[41]
KW-1 <sup>a</sup>		DMF	301 (4.58); 369 (3.51); 515 (3.56)	0.625	1.06	—	0.46	0.31	[57]
RT-1 <sup>a</sup>		DMF	301 (3.04); 368 (2.28); 529 (1.41)	0.58	6.0	—	0.70	2.45	[79]
RT-2 <sup>a</sup>		DMF	300 (4.34); 445 (2.88); 551 (1.68)	0.57	5.3	—	0.75	2.84	[79]
RT-3 <sup>a</sup>		DMF	305 (4.56); 388 (3.15); 563 (2.76)	0.54	4.5	—	0.76	1.85	[79]
(continued)									

(continued)

Table 3 (continued)

Abbreviation	Structure	Absorption properties		Photoelectrochemical performance					References
		Solvent	$\lambda_{MAX}/nm$ ( $\epsilon_{MAX}/10^4\text{ L mol}^{-1}\text{ cm}^{-1}$ )	$V_{OC}/V$	$J_{SC}/\text{mA cm}^{-2}$	IPCE <sub>MAX</sub> % ( $\lambda/nm$ )	$ff$	$\eta_{cell}$ %	
C107		DMF	310 (3.9); 453 (5.43); 552 (2.8)	0.739	19.8	92 (550)	0.751	10.7	[47]
SJW-E1		DMF	310; 360; 546 (1.87)	0.669	21.6	72.6 (550)	0.626	9.02	[77]

<sup>a</sup>These compounds were named after the initials of the first author of the reference cited

## 8.1 1,10-Phenanthroline Derivative Ligands

Besides 2,2'-bipyridine derivatives, 1,10-phenanthroline and its derivatives are gaining attention to be used in *cis*-[Ru(dcbH<sub>2</sub>)(L)(NCS)<sub>2</sub>] sensitizers. Their similarity to 2,2'-bipyridine and the advantage of having an extended  $\pi$ -conjugated structure led to a great potential to be employed as ancillary ligands [81]. This class of compounds still having few complexes reported in DSSCs, and their spectral as well as photoelectrochemical parameters are listed in Table 4.

The use of phenanthroline derivatives in ruthenium(II) sensitizers leads to properties favorable to the energy conversion processes and can increase the DSSCs performances, which have shown promising results [48, 82, 83].

The comparison on the properties of the complex NOK-1 [83] with N3 indicates that the substitution of the 2,2'-bipyridine derivative by 1,10-phenanthroline does not exhibit better performance or absorption properties. On the other hand, the complexes YS5 and AVM-2 exhibit higher absorbance and also had better performance than the complexes N719 and N3 under the same conditions [48, 86], indicating that this is a promising class of compounds to be investigated. Their higher efficiency was ascribed to an enhancement of electron injection. This effect is due to the reduction of dihedral angle between phenanthroline and its substituents (phenyl or carbazole) on the excited state, allowing the electron injection through the thermalized triplet excited state.

## 9 Natural Dyes

Faster, cheaper, low-energy way alternative for ruthenium sensitizers are natural dyes and these compounds have been gaining much attention. Natural dyes can be obtained from fruits, flowers, or leaves and are suitable for educational purposes [91–93] or are an environmentally friendly alternative for dye production since a long-term stability of DSSC using these sensitizers has been demonstrated [94].

On the last years, these natural dyes solar cells experienced a great transformation, focusing on alternatives to improve the performance of such DSSCs [95–102], and special attention is given for dye cocktails [103–106] or co-sensitization approach [107]. There are also several papers describing the use of natural dyes in solid, or quasi-solid, solar cells [108, 109] or using semiconductors such as ZnO [110–112] in such DSSCs, as well as their use on investigations of electron injection/recombination processes. In this chapter, it is presented only the results reported on natural dye-sensitizers used in DSSCs having TiO<sub>2</sub> as semiconductor and liquid mediator.

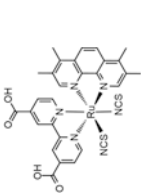
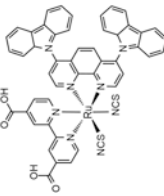
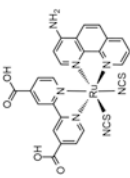
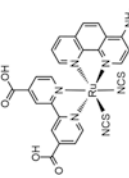
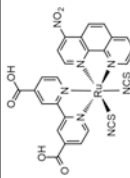
The absorption properties and photoelectrochemical performance of natural dye-sensitized solar cells reported since 2003 are listed in Table 5.

**Table 4** Absorption properties and photoelectrochemical performance of ruthenium(II) *tris*-heteroleptic ruthenium compounds having 1,10-phenanthroline derivatives

Abbreviation	Structure	Absorption properties		Photoelectrochemical performance					References
		Solvent	$\lambda_{MAX}/nm$ ( $\epsilon_{MAX}/10^4 L mol^{-1} cm^{-1}$ )	$V_{oc}/V$	$J_{sc}/mA cm^{-2}$	IPCE <sub>MAX</sub> % ( $\lambda/nm$ )	$ff$	$\eta_{cell}$ %	
Y55		DMF	283(5.68), 308 (3.95), 362 (0.81), 522 (1.71)	0.749	14.52	64.6 (540)	0.557	6.05	[48]
AR25		DMF	420; 518(6.58)	0.69	9.6	61 (520)	0.39	2.6	[82]
NOK-1 <sup>a</sup>		0.01 M NaOH aqueous solution	267 (5.7); 309 (2.9); 400 (1.0); 492(1.2)	0.65	15.3	74	0.67	6.7	[83]
NOK-2 <sup>a</sup>		0.01 M NaOH aqueous solution	275 (5.7); 310 (3.5); 374 (1.8); 492 (1.1)	0.62	11.7	54	0.73	5.3	[83]
FC-1 <sup>a</sup>		Acetonitrile	430 (1.3); 535 (1.0)	0.683	12.72	60 (515)	0.55	4.60	[84]

(continued)

Table 4 (continued)

Abbreviation	Structure	Absorption properties		Photoelectrochemical performance						References
		Solvent	$\lambda_{MAX}/nm$ ( $\epsilon_{MAX}/10^4\text{ L mol}^{-1}\text{ cm}^{-1}$ )	$V_{oc}/V$	$J_{sc}/\text{mA cm}^{-2}$	IPCE <sub>MAX</sub> % ( $\lambda/nm$ )	$ff$	$\eta_{cell}\%$		
AVM-1 <sup>a</sup>		Acetonitrile	420 (1.3); 535 (0.8)	0.627	11.9	50 (505)	0.67	5.0	[85]	
AVM-2 <sup>a</sup>		Ethanol	330 (2.0); 375 (1.4); 525 (1.8)	0.76	15.6	79 (500)	0.716	8.6	[86]	
AR24a		DMF	420 (1.2); 546 (0.9)	0.48	1.45	—	0.31	0.22	[87]	
AR24b		DMF	415 (1.0); 545 (0.9)	0.46	0.98	—	0.31	0.14	[87]	
AR27a		DMF	403 (0.5); 538 (0.7)	0.44	5.26	—	0.34	0.8	[87]	

(continued)

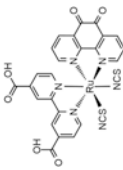
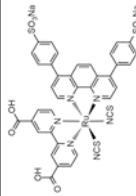
Table 4 (continued)

Abbreviation	Structure	Absorption properties		Photoelectrochemical performance					References
		Solvent	$\lambda_{MAX}/nm$ ( $\epsilon_{MAX}/10^4 L mol^{-1} cm^{-1}$ )	$V_{oc}/V$	$J_{sc}/mA cm^{-2}$	IPCE <sub>MAX</sub> % ( $\lambda/nm$ )	$ff$	$\eta_{cell}$ %	
AR27b		DMF	400 (0.5); 535 (0.7)	0.44	0.79	—	0.35	0.13	[87]
HJ1		Methanol	304 (1.33); 428 (0.52), 516 (0.57)	0.67	9.65	—	0.44	2.83	[88]
CYC-P1		DMF	302 (3.9); 380 (3.8); 518 (0.8)	0.64	14.92	—	0.63	6.01	[89]
CYC-P2		DMF	304 (2.3); 423 (2.2); 530 (0.4)	0.55	9.8	—	0.64	3.42	[89]

(continued)



Table 4 (continued)

Abbreviation	Structure	Absorption properties		Photoelectrochemical performance						References
		Solvent	$\lambda_{MAX}/nm$ ( $\epsilon_{MAX}/10^4\text{ L mol}^{-1}\text{ cm}^{-1}$ )	$V_{OC}/V$	$J_{SC}/\text{mA cm}^{-2}$	IPCE <sub>MAX</sub> % ( $\lambda/nm$ )	$ff$	$\eta_{cell}\%$		
K27		DMF	292 (4.8); 380 (1.3); 524 (1.1)	0.55	7.19	—	0.63	2.51	[90]	
K28		DMF	308 (5.4); 380 (1.0); 476 (1.6); 522 (1.8)	0.50	5.59	—	0.60	1.69	[90]	

<sup>a</sup>These compounds were named after the initials of the first author of the reference cited

**Table 5** Absorption properties and photoelectrochemical performance of natural dye-sensitized solar cells reported since 2003

Extract of	Dye	Medium	$\lambda_{\text{max}}$ (nm)	$V_{\text{oc}}/V$	$J_{\text{sc}}$ (mA cm <sup>-2</sup> )	$ff$	$\eta_{\text{cell}}$ (%)	References
Red cabbage	Anthocyanin	Water	550	0.52	0.68	0.70	0.50	[113]
Rosella flower ( <i>Hibiscus sabdariffa</i> L.)	Anthocyanin	Water	520	0.404	1.63	0.57	0.37	[114]
Blue pea flower ( <i>Clitoria tematea</i> )	Anthocyanin	Water	580, 620	0.372	0.37	0.33	0.05	[114]
<i>Canna indica</i> flower	Anthocyanin	Water and Ethanol	513	0.54	0.82	0.59	0.29	[115]
		TiO <sub>2</sub>	530	—	—	—	—	
<i>Salvia splendens</i> flower	Anthocyanin	Water and ethanol	507	0.558	0.7	0.61	0.26	[115]
		TiO <sub>2</sub>	516	—	—	—	—	
Cowberry	Anthocyanin	Water and ethanol	522	0.556	0.4	0.54	0.13	[115]
		TiO <sub>2</sub>	531	—	—	—	—	
<i>Solanum nigrum</i>	Anthocyanin	Water and ethanol	539	0.54	1.01	0.51	0.31	[115]
		TiO <sub>2</sub>	564	—	—	—	—	
<i>Rhododendron arboretum zeylanicum</i>	Anthocyanin	Ethanol	538	0.4020	1.15	0.637	0.29	[116]
<i>Sesbania grandiflora</i> Scarlet	Anthocyanin	Ethanol	544	0.4067	4.40	0.569	1.02	[116]
<i>Hibiscus rosasinensis</i>	Anthocyanin	Ethanol	534	0.4003	4.04	0.633	1.02	[116]
<i>Hibiscus surattensis</i>	Anthocyanin	Ethanol	545	0.3921	5.45	0.535	1.14	[116]
<i>Nerium oleander</i>	Anthocyanin	Ethanol	539	0.4088	2.46	0.591	0.59	[116]
<i>Ixora macrothyrsa</i>	Anthocyanin	Ethanol	537	0.4031	1.31	0.568	0.30	[116]
Black rice ( <i>Oryza sativa</i> L. indica)	Anthocyanin	Ethanol	560	0.551	1.142	0.52	—	[117]
<i>Rosa xanthina</i>	Anthocyanin	Ethanol	560	0.492	0.637	0.52	—	[117]
Maple leaves	Anthocyanin	Ethanol	536	0.65	1.0	0.60	0.4	[118]
Red Sicilian orange	Anthocyanin	Water	515	0.340	3.84	0.5	—	[119]
Skin of eggplant	Anthocyanin	Water	522	0.350	3.40	0.4	—	[119]
Skin of jaboricaba	Anthocyanin	Ethanol	535	0.66	2.6	0.62	—	[120]
Begonia	Anthocyanin	Ethanol	540	0.537	0.63	0.722	0.24	[121]

(continued)

Table 5 (continued)

Extract of	Dye	Medium	$\lambda_{\text{max}}$ (nm)	$V_{\text{oc}}/V$	$J_{\text{sc}}$ (mA cm <sup>-2</sup> )	$ff$	$\eta_{\text{cell}}$ (%)	References
Violet	Anthocyanin	0.1 M HCl— ethanol	546	0.498	1.02	0.645	0.33	[121]
Blackberry	Anthocyanin	—	—	0.320	5.85	0.57	1.07	[122]
Mulberry	Anthocyanin	TiO <sub>2</sub>	553	0.42	0.86	0.43	—	[123]
Red mulberry	Anthocyanin	—	—	0.340	4.45	0.64	0.99	[122]
Radicchio	Anthocyanin	—	—	0.322	5.05	0.55	0.90	[122]
Giacchè grapes	Anthocyanin	—	—	0.333	3.06	0.56	0.57	[122]
<i>Erythrina variegata</i>	Anthocyanin	Ethanol	451; 492	0.48	0.78	0.55	—	[124]
Chaste tree fruit	Anthocyanin	TiO <sub>2</sub>	555	0.39	1.06	0.48	—	[123]
Cabbage-palm fruit	Anthocyanin	TiO <sub>2</sub>	552	0.44	0.37	0.61	—	[123]
Dragon fruit ( <i>Hylocereus polyrhizus</i> )	Anthocyanin	Water	535	0.22	0.20	0.30	0.22	[125]
Bitter leaf ( <i>Vernonia amygdalin</i> )	Anthocyanin	Ethanol	400	0.38	0.50	0.89	0.96	[126]
Red onion ( <i>Allium cepa</i> )	Anthocyanin	Water	520	0.44	0.51	0.48	0.14	[127]
Henna ( <i>Lawsonia inermis</i> )	Anthocyanin	Ethanol	518	0.61	1.87	0.58	0.66	[128]
Red frangipani flowers	Anthocyanin	Ethanol	530	0.50	0.94	0.65	0.301	[129]
<i>R. chinensis</i>	Anthocyanin	—	—	0.54	0.80	0.66	0.29	[130]
<i>Delonix regia</i>	Anthocyanin	TiO <sub>2</sub>	538	0.30	1.33	0.39	0.317	[131]
<i>Eugenia jambolana</i>	Anthocyanin	TiO <sub>2</sub>	543	0.35	1.49	0.48	0.505	[131]
<i>Panica granatum pleniflora</i>	Anthocyanin	—	—	0.62	0.40	0.61	0.15	[132]
<i>Consolida orientalis</i>	Anthocyanin	—	—	0.60	0.56	0.53	0.18	[132]
<i>Clematis orientalis</i>	Anthocyanin	—	—	0.42	0.22	0.49	0.05	[132]
Strawberry	Anthocyanin	—	—	0.47	1.33	0.37	0.229	[133]
<i>Luffa cylindrica L.</i>	Anthocyanin	Ethanol	420; 450	0.52	0.44	0.60	0.13	[134]
Purple corn (husk)	Anthocyanin	—	—	0.46	3.57	0.64	1.06	[135]

(continued)

Table 5 (continued)

Extract of	Dye	Medium	$\lambda_{\text{max}}$ (nm)	$V_{\text{oc}}/V$	$J_{\text{sc}}$ (mA cm <sup>-2</sup> )	$ff$	$\eta_{\text{cell}}$ (%)	References
Purple corn (cob)	Anthocyanin	—	—	0.48	3.42	0.62	1.01	[135]
Purple corn (silk)	Anthocyanin	—	—	0.48	3.25	0.62	0.96	[135]
Red tamarind ( <i>T. indica</i> )	Anthocyanin	Methanol	525	0.532	0.35	0.67	0.14	[136]
Calafate fruit	Anthocyanin	Water	525	0.47	6.2	0.36	—	[120]
		TiO <sub>2</sub>	545	—	—	—	—	
Raw beet	Betalain	TiO <sub>2</sub>	470	0.22	2.00	0.51	0.19	[137]
		Water	535	—	—	—	—	
Red turnip	Betalain	Water	484, 536	0.425	9.5	0.37	1.7	[138]
		TiO <sub>2</sub>	450	—	—	—	—	
Wild silician prickly pear	Betalain	TiO <sub>2</sub>	460	0.375	8.20	0.38	1.19	[138]
Red <i>Bougainvillea glabra</i>	Betalain	Water	482, 535	0.26	2.34	0.74	0.45	[139]
Violet <i>Bougainvillea glabra</i>	Betalain	Water	547	0.23	1.86	0.71	0.31	[139]
Red <i>Bougainvillea spectabilis</i>	Betalain	Water	480	0.28	2.29	0.76	0.48	[139]
Violet <i>Bougainvillea spectabilis</i>	Betalain	Water	535	0.25	1.88	0.73	0.35	[139]
Cactus fruits ( <i>O. dillenii</i> )	Betalain	Methanol	517	0.521	1.09	0.69	0.47	[136]
Kelp	Chlorophyll	Ethanol	460	0.441	0.433	0.62	—	[117]
Wormwood	Chlorophyll	Ethanol	432	0.67	2.3	0.56	0.9	[118]
Bamboo leaves	Chlorophyll	Ethanol	432	0.67	1.9	0.56	0.7	[118]
Pomegranate leaves	Chlorophyll	Ethanol	412, 665	0.560	2.05	0.52	0.597	[140]
Perilla	Chlorophyll	Ethanol	665	0.522	1.36	0.696	0.50	[121]
Petunia	Chlorophyll	Ethanol	665	0.616	0.85	0.605	0.32	[121]
China loropetal	Chlorophyll	Ethanol	665	0.518	0.84	0.626	0.27	[121]
Chinese rose	Chlorophyll	0.1 M HCl— ethanol	516	0.483	0.90	0.619	0.27	[121]

(continued)

Table 5 (continued)

Extract of	Dye	Medium	$\lambda_{\text{max}}$ (nm)	$V_{\text{oc}}/V$	$J_{\text{sc}}$ (mA cm <sup>-2</sup> )	$ff$	$\eta_{\text{cell}}$ (%)	References
Spinach	Chlorophyll	Ethanol	437	0.55	0.47	0.51	0.131	[141]
Ipomoea	Chlorophyll	Ethanol	410	0.54	0.91	0.56	0.278	[141]
<i>Festuca ovina</i>	Chlorophyll	Methanol	420; 660	0.54	1.18	0.69	0.46	[142]
Shiso	Chlorophyll	Water and Ethanol	440; 600	0.55	3.56	0.51	1.01	[143]
<i>Ficus reusa</i>	Chlorophyll	Ethanol	670	0.520	7.85	0.29	1.18	[144]
<i>Rhoeo spathacea</i>	Chlorophyll	Ethanol	670	0.496	10.9	0.27	1.49	[144]
<i>Garcinia subelliptica</i>	Chlorophyll	Ethanol	670	0.322	6.48	0.33	0.691	[144]
<i>Aneithum graveolens</i>	Chlorophyll	Ethanol	666	0.579	0.965	0.40	0.22	[145]
Parsley ( <i>Petroselinum crispum</i> )	Chlorophyll	Ethanol	666	0.445	0.535	0.34	0.07	[145]
Arugula	Chlorophyll	Ethanol	666	0.599	0.788	0.42	0.20	[145]
Green algae	Chlorophyll	Ethanol	666	0.559	0.397	0.44	0.10	[145]
<i>U. pinnatifida</i>	Chlorophyll	—	—	0.36	0.8	0.69	0.178	[146]
Curcumin	Polyphenol	Ethanol	430	0.53	0.53	0.72	0.41	[113]
Tangerine peel	Polyphenol	Ethanol	446	0.592	0.74	0.631	0.28	[121]
Flowery knotweed	Polyphenol	Ethanol	435	0.554	0.60	0.627	0.21	[121]
<i>Reseda luteola</i>	Polyphenol	—	—	0.64	0.54	0.64	0.22	[132]
<i>Berberis integerrima</i>	Polyphenol	—	—	0.56	0.004	0.53	0.01	[132]
<i>Reseda gredensis</i>	Polyphenol	—	—	0.53	0.14	0.71	0.07	[132]
<i>Consolida ajacis</i>	Polyphenol	—	—	0.55	1.68	0.65	0.60	[132]
<i>Salvia sclarea</i>	Polyphenol	—	—	0.37	0.10	0.54	0.02	[132]
Mallow	Polyphenol	Ethanol	660	0.60	0.69	0.55	0.215	[133]
Erythrina	Carotenoid	Ethanol	451	0.484	0.776	0.55	—	[117]
Capsicum	Carotenoid	Ethanol	455	0.412	0.225	0.63	—	[117]
Achiote seed	Carotenoid	Chloroform	440, 475, 500	0.56	0.53	0.66	0.19	[147]

(continued)

Table 5 (continued)

Extract of	Dye	Medium	$\lambda_{\text{max}}$ (nm)	$V_{\text{oc}}/V$	$J_{\text{sc}}$ (mA cm <sup>-2</sup> )	$ff$	$\eta_{\text{cell}}$ (%)	References
Fructus lycii	Carotenoid	Ethanol	447; 425	0.689	0.53	0.466	0.17	[121]
Marigold	Carotenoid	Ethanol	487	0.542	0.51	0.831	0.23	[121]
Yellow rose	Carotenoid	Ethanol	487	0.609	0.74	0.571	0.26	[121]
Ivy gourd fruits	Carotenoid	Ethanol	458; 480	0.64	0.24	0.49	0.076	[129]
<i>K. japonica</i>	Carotenoid	—	—	0.59	0.56	0.68	0.22	[130]
<i>Adonis flammæa</i>	Carotenoid	—	—	0.59	0.40	0.66	0.16	[132]
Red perilla	—	—	—	0.51	0.39	0.67	0.27	[113]
Herba artemisiae scopariae	—	Ethanol	669	0.484	1.03	0.682	0.34	[121]
Bauhinia tree	—	Ethanol	665	0.572	0.96	0.660	0.36	[121]
Lithospermum	—	Ethanol	520	0.337	0.14	0.585	0.03	[121]
Mangosteen pericarp	—	Ethanol	—	0.686	2.69	0.633	1.17	[121]
Rose	—	Water	—	0.595	0.97	0.659	0.38	[121]
Lily	—	Water	—	0.498	0.51	0.667	0.17	[121]
Coffee	—	Water	—	0.559	0.85	0.687	0.33	[121]
Broadleaf holly leaf	—	Water	—	0.607	1.19	0.654	0.47	[121]

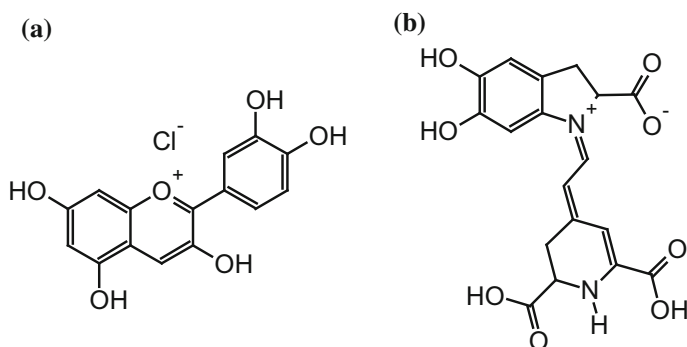


**Fig. 6** Structure of anthocyanidin (a), a flavinic ion of anthocyanin, and betanidin (b), a betalain compound

The most investigated classes of natural dyes are the anthocyanins, commonly found in red-purplish fruits or flowers; or betalains, Fig. 6. Besides these compounds, other sensitizers have also been investigated [148].

Betalain from raw beet, red turnip, and wild sicilian prickly pear have also been used as natural sensitizers and they have presented a good photoelectrochemical response, however these cells have low  $V_{OC}$ , with overall efficiency up to 1.7% and reasonable stability [138]. It was also observed the improvement on the photoelectrochemical performance due to changes on pH as well as in the presence of additives in the mediator layer [122].

Other classes of natural dyes, such as chlorophyll, polyphenol, etc., were also investigated, but the photoelectrochemical parameters were not as good as those observed for anthocyanins or betalains. Several reviews were published and describe the performance of these other classes of dyes along to those presented here [149–153].

## 10 Conclusion

The energy needs will be supplied by alternative sources and dye-sensitized solar cells are one of the most promising devices for this application since they are cheap and environmentally friendly. The investigation of dye-sensitizers is fundamental issue on the development of these devices and one of the most promising alternatives is the use of ruthenium *tris*-heteroleptic dyes sensitizers to modulate or enhance their photoelectrochemical performance. The investigation on natural extracts to be employed as dye-sensitizers has also been attracting much attention in the last years. They can be an alternative to further reduction of the production costs of these revolutionary devices.

**Acknowledgements** The authors would like to acknowledge to CNPq, FAPESP, and CAPES for financial support.

## References

1. Cook TR et al (2010) Solar energy supply and storage for the legacy and nonlegacy worlds. *Chem Rev* 110(11):6474–6502
2. Nocera DG (2009) Chemistry of personalized solar energy. *Inorg Chem* 48(21):10001–10017
3. Carrette L, Friedrich KA, Stimming U (2000) Fuel cells: principles, types, fuels, and applications. *Chem Phys Chem* 1(4):162–193
4. Cameron D, Holliday R, Thompson D (2003) Gold's future role in fuel cell systems. *J Power Sources* 118(1–2):298–303
5. Lemos SG et al (2007) Electrocatalysis of methanol, ethanol and formic acid using a Ru/Pt metallic bilayer. *J Power Sour* 163(2):695–701
6. Freitas RG et al (2007) Methanol oxidation reaction on  $\text{Ti/RuO}_{2(x)}\text{Pt}_{(1-x)}$  electrodes prepared by the polymeric precursor method. *J Power Sour* 171(2):373–380
7. Polo AS et al (2011) Pt-Ru-TiO<sub>2</sub> photoelectrocatalysts for methanol oxidation. *J Power Sour* 196(2):872–876
8. Gu C, Shannon C (2007) Investigation of the photocatalytic activity of TiO<sub>2</sub>-polyoxometalate systems for the oxidation of methanol. *J Mol Catal A: Chem* 262(1–2):185–189
9. Drew K et al (2005) Boosting fuel cell performance with a semiconductor photocatalyst: TiO<sub>2</sub>/Pt-Ru hybrid catalyst for methanol oxidation. *J Phys Chem B* 109(24):11851–11857
10. Kamat PV (2007) Meeting the clean energy demand: nanostructure architectures for solar energy conversion. *J Phys Chem C* 111(7):2834–2860
11. Armaroli N, Balzani V (2007) The future of energy supply: challenges and opportunities. *Angew Chem Int Ed Engl* 46(1–2):52–66
12. Meyer TJ (1989) Chemical approaches to artificial photosynthesis. *Acc Chem Res* 22(5):163–170
13. Dubois MR, Dubois DL (2009) Development of molecular electrocatalysts for CO<sub>2</sub> reduction and H<sub>2</sub> production/oxidation. *Acc Chem Res* 42(12):1974–1982
14. Morris AJ, Meyer GJ, Fujita E (2009) Molecular approaches to the photocatalytic reduction of carbon dioxide for solar fuels. *Acc Chem Res* 42(12):1983–1994
15. Concepcion JJ et al (2009) Making oxygen with ruthenium complexes. *Acc Chem Res* 42(12):1954–1965
16. Walter MG et al (2010) Solar water splitting cells. *Chem Rev* 110(11):6446–6473
17. Caramori S et al (2010) Photoelectrochemical behavior of sensitized TiO<sub>2</sub> photoanodes in an aqueous environment: application to hydrogen production. *Inorg Chem* 49(7):3320–3328
18. Koike K et al (2009) Architecture of supramolecular metal complexes for photocatalytic CO<sub>2</sub> reduction: III: effects of length of alkyl chain connecting photosensitizer to catalyst. *J Photochem Photobiol, A* 207(1):109–114
19. Takeda H et al (2008) Development of an efficient photocatalytic system for CO<sub>2</sub> reduction using rhenium(I) complexes based on mechanistic studies. *J Am Chem Soc* 130(6):2023–2031
20. Kroon JM et al (2007) Nanocrystalline dye-sensitized solar cells having maximum performance. *Prog Photovoltaics Res Appl* 15(1):1–18
21. Tributsch H (1972) Reaction of excited chlorophyll molecules at electrodes and in photosynthesis. *Photochem Photobiol* 16(4):261–269
22. O'Regan B, Gratzel M (1991) A low-cost, high-efficiency solar cell based on dye-sensitized colloidal TiO<sub>2</sub> films. *Nature* 353(6346):737–740



23. Grätzel M (2001) Photoelectrochemical cells. *Nature* 414(6861):338–344
24. Katoh R et al (2004) Kinetics and mechanism of electron injection and charge recombination in dye-sensitized nanocrystalline semiconductors. *Coord Chem Rev* 248(13–14):1195–1213
25. Gregg BA (2004) Interfacial processes in the dye-sensitized solar cell. *Coord Chem Rev* 248(13–14):1215–1224
26. Galoppini E (2004) Linkers for anchoring sensitizers to semiconductor nanoparticles. *Coord Chem Rev* 248(13–14):1283–1297
27. Anderson NA, Lian T (2004) Ultrafast electron injection from metal polypyridyl complexes to metal-oxide nanocrystalline thin films. *Coord Chem Rev* 248(13–14):1231–1246
28. Asbury JB et al (2003) Parameters affecting electron injection dynamics from ruthenium dyes to titanium dioxide nanocrystalline thin film. *J Phys Chem B* 107(30):7376–7386
29. Anderson NA, Ai X, Lian T (2003) Electron injection dynamics from Ru polypyridyl complexes to ZnO nanocrystalline thin films. *J Phys Chem B* 107(51):14414–14421
30. Garcia CG et al (2002) Electron injection versus charge recombination in photoelectrochemical solar cells using  $\text{cis}[(\text{dcbH}_2)_2\text{Ru}(\text{CNpy})(\text{H}_2\text{O})]\text{Cl}_2$  as a nanocrystalline  $\text{TiO}_2$  sensitizer. *J Photochem Photobiol, A* 151(1–3):165–170
31. Garcia CG et al (2002) Time-resolved experiments in dye-sensitized solar cells using  $[(\text{dcbH}_2)_2\text{Ru}(\text{ppy})_2](\text{ClO}_4)_2$  as a nanocrystalline  $\text{TiO}_2$  sensitizer. *J Photochem Photobiol, A* 147(2):143–148
32. Kuang DB et al (2006) High molar extinction coefficient heteroleptic ruthenium complexes for thin film dye-sensitized solar cells. *J Am Chem Soc* 128(12):4146–4154
33. Wang P et al (2004) Stable new sensitizer with improved light harvesting for nanocrystalline dye-sensitized solar cells. *Adv Mater* 16(20):1806
34. Wang P et al (2004) Amphiphilic polypyridyl ruthenium complexes with substituted 2,2'-dipyridylamine ligands for nanocrystalline dye-sensitized solar cells. *Chem Mater* 16(17):3246–3251
35. Pelet S, Moser J-E, Gratzel M (2000) Cooperative effect of adsorbed cations and iodide on the interception of back electron transfer in the dye sensitization of nanocrystalline  $\text{TiO}_2$ . *J Phys Chem B* 104(8):1791–1795
36. Patrocinio AOT, Paterno LG, Iha NYM (2010) Role of polyelectrolyte for layer-by-layer compact  $\text{TiO}_2$  films in efficiency enhanced dye-sensitized solar cells. *J Phys Chem C* 114(41):17954–17959
37. Murakami Iha NY, Arcia CG, Bignozzi CA (2003) Dye-sensitized photoelectrochemical solar cells. In: Nalwa HS (ed) *Handbook of photochemistry and photobiology*. American Scientific Publishers, Stevenson Ranch, California, USA, pp 49–82
38. Nazeeruddin MK et al (1993) Conversion of light to electricity by  $\text{cis-X}_2\text{bis}(2,2'\text{-bipyridyl-4,4'-dicarboxylate})\text{ruthenium(II)}$  charge-transfer sensitizers ( $\text{X} = \text{Cl}^-$ ,  $\text{Br}^-$ ,  $\text{I}^-$ ,  $\text{CN}^-$ , and  $\text{SCN}^-$ ) on nanocrystalline  $\text{TiO}_2$  electrodes. *J Am Chem Soc* 115(14):6382–6390
39. Nazeeruddin MK, Gratzel M (2001) Separation of linkage isomers of trithiocyanato (4,4',4''-tricarboxy-2,2',6,2''-terpyridine)ruthenium(II) by pH-titration method and their application in nanocrystalline  $\text{TiO}_2$ -based solar cells. *J Photochem Photobiol A-Chem* 145(1–2):79–86
40. Chen CY et al (2006) A ruthenium complex with superhigh light-harvesting capacity for dye-sensitized solar cells. *Angewandte Chem Int Ed* 45(35):5822–5825
41. Cao YM et al (2009) Dye-sensitized solar cells with a high absorptivity ruthenium sensitizer featuring a 2-(Hexylthio)thiophene conjugated bipyridine. *J Phys Chem C* 113(15):6290–6297
42. Nazeeruddin MK et al (2003) Investigation of sensitizer adsorption and the influence of protons on current and voltage of a dye-sensitized nanocrystalline  $\text{TiO}_2$  solar cell. *J Phys Chem B* 107(34):8981–8987
43. Lv XJ, Wang FF, Li YH (2010) Studies of an extremely high molar extinction coefficient ruthenium sensitizer in dye-sensitized solar cells. *ACS Appl Mater Interfaces* 2(7):1980–1986

44. Gao F et al (2008) Enhance the optical absorptivity of nanocrystalline  $\text{TiO}_2$  film with high molar extinction coefficient ruthenium sensitizers for high performance dye-sensitized solar cells. *J Am Chem Soc* 130(32):10720–10728
45. Chen CY et al (2009) Highly efficient light-harvesting ruthenium sensitizer for thin-film dye-sensitized solar cells. *ACS Nano* 3(10):3103–3109
46. Chen CY et al (2009) New ruthenium sensitizer with carbazole antennas for efficient and stable thin-film dye-sensitized solar cells. *J Phys Chem C* 113(48):20752–20757
47. Yu QJ et al (2009) An extremely high molar extinction coefficient ruthenium sensitizer in dye-sensitized solar cells: the effects of pi-conjugation extension. *J Phys Chem C* 113(32):14559–14566
48. Sun YL et al (2010) Viable alternative to N719 for dye-sensitized solar cells. *ACS Appl Mater Interfaces* 2(7):2039–2045
49. Polo AS, Itokazu MK, Murakami Iha NY (2004) Metal complex sensitizers in dye-sensitized solar cells. *Coord Chem Rev* 248(13–14):1343–1361
50. Pashaei B et al (2016) Influence of ancillary ligands in dye-sensitized solar cells. *Chem Rev* 116(16):9485–9564
51. Jin Zhengzhe et al (2008) Triarylamine-functionalized ruthenium dyes for efficient dye-sensitized solar cells. *Chem Sus Chem* 1(11):901–904
52. Mitsopoulou CA et al (2007) Synthesis, characterization and sensitization properties of two novel mono and bis carboxyl-dipyrido-phenazine ruthenium(II) charge transfer complexes. *J Photochem Photobiol A-Chem* 191:6–12
53. Huang WK et al (2010) Synthesis and electron-transfer properties of benzimidazole-functionalized ruthenium complexes for highly efficient dye-sensitized solar cells. *Chem Commun* 46(47):8992–8994
54. Wu SJ et al (2010) An efficient light-harvesting ruthenium dye for solar cell application. *Dyes Pigm* 84(1):95–101
55. Abbotto A et al (2008) Electron-rich heteroaromatic conjugated bipyridine based ruthenium sensitizer for efficient dye-sensitized solar cells. *Chem Commun* 42:5318–5320
56. Yum JH et al (2009) High efficient donor-acceptor ruthenium complex for dye-sensitized solar cell applications. *Energy Environ Sci* 2(1):100–102
57. Willinger K et al (2009) Synthesis, spectral, electrochemical and photovoltaic properties of novel heteroleptic polypyridyl ruthenium(II) donor-antenna dyes. *J Mater Chem* 19(30):5364–5376
58. Wang P et al (2003) A stable quasi-solid-state dye-sensitized solar cell with an amphiphilic ruthenium sensitizer and polymer gel electrolyte (vol 2, p 402, 2003). *Nat Mater* 2(7):498
59. Sahin C et al (2008) Synthesis of an amphiphilic ruthenium complex with swallow-tail bipyridyl ligand and its application in nc-DSC. *Inorg Chim Acta* 361(3):671–676
60. Nazeeruddin MK et al (2004) Stepwise assembly of amphiphilic ruthenium sensitizers and their applications in dye-sensitized solar cell. *Coord Chem Rev* 248(13–14):1317–1328
61. Klein C et al (2004) Amphiphilic ruthenium sensitizers and their applications in dye-sensitized solar cells. *Inorg Chem* 43(14):4216–4226
62. Gao FF et al (2008) A new heteroleptic ruthenium sensitizer enhances the absorptivity of mesoporous titania film for a high efficiency dye-sensitized solar cell. *Chem Commun* 23:2635–2637
63. Hallett AJ, Jones JE (2011) Purification-free synthesis of a highly efficient ruthenium dye complex for dye-sensitized solar cells (DSSCs). *Dalton Trans* 40(15):3871–3876
64. Lagref JJ, Nazeeruddin MK, Grätzel M (2003) Molecular engineering on semiconductor surfaces: design, synthesis and application of new efficient amphiphilic ruthenium photosensitizers for nanocrystalline  $\text{TiO}_2$  solar cells. *Synth Met* 138(1–2):333–339
65. Sygkridou D et al (2015) Comparative studies of pyridine and bipyridine ruthenium dye complexes with different side groups as sensitizers in sol-gel quasi-solid-state dye sensitized solar cells. *Electrochim Acta* 160:227–234
66. Kong F-T, Dai S-Y, Wang K-J (2007) New amphiphilic polypyridyl ruthenium(II) sensitizer and its application in dye-sensitized solar cells. *Chin J Chem* 25(2):168–171

67. Liu K-Y et al (2010) Synthesis and characterization of cross-linkable ruthenium complex dye and its application on dye-sensitized solar cells. *J Polym Sci, Part A: Polym Chem* 48 (2):366–372
68. Ni J-S et al (2012) Effects of tethering alkyl chains for amphiphilic ruthenium complex dyes on their adsorption to titanium oxide and photovoltaic properties. *J Colloid Interface Sci* 386 (1):359–365
69. Song Y-Y et al (2009) Amphiphilic TiO<sub>2</sub> nanotube arrays: an actively controllable drug delivery system. *J Am Chem Soc* 131(12):4230–4232
70. Giribabu L et al (2009) High molar extinction coefficient amphiphilic ruthenium sensitizers for efficient and stable mesoscopic dye-sensitized solar cells. *Energy Environ Sci* 2(7):770–773
71. Jiang KJ et al (2008) Efficient sensitization of nanocrystalline TiO<sub>2</sub> films with highmolar extinction coefficient ruthenium complex. *Inorg Chim Acta* 361(3):783–785
72. Gao FF et al (2009) Conjugation of selenophene with bipyridine for a high molar extinction coefficient sensitizer in dye-sensitized solar cells. *Inorg Chem* 48(6):2664–2669
73. Nazeeruddin MK et al (2007) A high molar extinction coefficient charge transfer sensitizer and its application in dye-sensitized solar cell. *J Photochem Photobiol A Chem* 185(2–3):331–337
74. Karthikeyan CS et al (2007) Highly efficient solid-state dye-sensitized TiO<sub>2</sub> solar cells via control of retardation of recombination using novel donor-antenna dyes. *Sol Energy Mater Sol Cells* 91(5):432–439
75. Kuang D et al (2007) High-efficiency and stable mesoscopic dye-sensitized solar cells based on a high molar extinction coefficient ruthenium sensitizer and nonvolatile electrolyte. *Adv Mater* 19(8):1133–1137
76. Hussain M et al (2013) Structure-property relationship of extended [small pi]-conjugation of ancillary ligands with and without an electron donor of heteroleptic Ru(II) bipyridyl complexes for high efficiency dye-sensitized solar cells. *Phys Chem Chem Phys* 15 (21):8401–8408
77. Chen CY et al (2007) A new route to enhance the light-harvesting capability of ruthenium complexes for dye-sensitized solar cells. *Adv Mater* 19(22):3888
78. Li J-Y et al (2010) Heteroleptic ruthenium antenna-dye for high-voltage dye-sensitized solar cells. *J Mater Chem* 20(34):7158–7164
79. Ryu TI et al (2009) Synthesis and photovoltaic properties of novel ruthenium(II) sensitizers for dye-sensitized solar cell applications. *Bull Korean Chem Soc* 30(10):2329–2337
80. Zhu SS, Kingsborough RP, Swager TM (1999) Conducting redox polymers: investigations of polythiophene-Ru(bpy)<sub>3</sub>(3)(n<sup>+</sup>) hybrid materials. *J Mater Chem* 9(9):2123–2131
81. Hara K et al (2001) Dye-sensitized nanocrystalline TiO<sub>2</sub> solar cells based on ruthenium(II) phenanthroline complex photosensitizers. *Langmuir* 17(19):5992–5999
82. Reynal A et al (2008) A phenanthroline heteroleptic ruthenium complex and its application to dye-sensitized solar cells. *Eur J Inorg Chem* 12:1955–1958
83. Onozawa-Komatsuzaki N et al (2006) Molecular and electronic ground and excited structures of heteroleptic ruthenium polypyridyl dyes for nanocrystalline TiO<sub>2</sub> solar cells. *New J Chem* 30(5):689–697
84. Carvalho F et al (2014) Synthesis, characterization and photoelectrochemical performance of a Tris-heteroleptic ruthenium(II) complex having 4,7-dimethyl-1, 10-phenanthroline. *Inorg Chim Acta* 414:145–152
85. Müller AV et al (2015) Effects of methyl-substituted phenanthrolines on the performance of ruthenium(II) dye-sensitizers. *J Braz Chem Soc* 26(11):2224–2232
86. Muller AV et al (2016) A high efficiency ruthenium(II) Tris-heteroleptic dye containing 4,7-dicarbazole-1,10-phenanthroline for nanocrystalline solar cells. *Rsc Adv* 6(52):46487–46494
87. Reynal A et al (2008) Interfacial charge recombination between e<sup>-</sup>-TiO<sub>2</sub> and the  $\Gamma/I_3^-$  electrolyte in ruthenium heteroleptic complexes: dye molecular structure-open circuit voltage relationship. *J Am Chem Soc* 130(41):13558–13567

88. Oh H et al (2014) Synthesis of heteroleptic Ru(II) complexes ligated with 1,3-dihydro-1,1,3,3-tetramethyl-7,8-diazacyclopenta 1 phenanthren-2-one and application in dye-sensitized solar cells. *Synth Met* 198:260–266
89. Chen CY et al (2007) New ruthenium complexes containing oligoalkylthiophene-substituted 1,10-phenanthroline for nanocrystalline dye-sensitized solar cells. *Adv Func Mater* 17(1):29–36
90. Ocakoglu K et al (2012) The photovoltaic performance of new ruthenium complexes in DSSCs based on nanorod ZnO electrode. *Synth Met* 162(23):2125–2133
91. Smestad GP, Grätzel M (1998) Demonstrating electron transfer and nanotechnology: a natural dye-sensitized nanocrystalline energy converter. *J Chem Edu* 75(6):752–756
92. Smestad GP (1998) Education and solar conversion: demonstrating electron transfer. *Sol Energy Mater Sol Cells* 55(1–2):157–178
93. Sonai GG et al (2015) Solar cells sensitized with natural dyes: an introductory experiment about solar energy for undergraduate students. *Quim Nova* 38(10):1357–1365
94. Patrocinio AOT, Iha NYM (2010) Toward sustainability: solar cells sensitized by natural extracts. *Quim Nova* 33(3):574–578
95. Chien CY, Hsu BD (2013) Optimization of the dye-sensitized solar cell with anthocyanin as photosensitizer. *Solar Energy Part C* 98:203–211
96. Suyitno S et al (2015) Stability and efficiency of dye-sensitized solar cells based on papaya-leaf dye. *Spectrochim Acta Part A Mol Biomol Spectrosc* 148:99–104
97. Chien CY, Hsu BD (2014) Performance enhancement of dye-sensitized solar cells based on anthocyanin by carbohydrates. *Sol Energy* 108:403–411
98. Treat NA, Knorr FJ, McHale JL (2016) Templated assembly of betanin chromophore on TiO<sub>2</sub>: aggregation-enhanced light-harvesting and efficient electron injection in a natural dye-sensitized solar cell. *J Phys Chem C* 120(17):9122–9131
99. Teoli F et al (2016) Role of pH and pigment concentration for natural dye-sensitized solar cells treated with anthocyanin extracts of common fruits. *J Photochem Photobiol A Chem* 316:24–30
100. Akila Y et al (2016) Enhanced performance of natural dye sensitized solar cells fabricated using rutile TiO<sub>2</sub> nanorods. *Opt Mater* 58:76–83
101. Ananth S et al (2016) Enhanced photovoltaic behavior of dye sensitized solar cells fabricated using pre dye treated titanium dioxide nanoparticles. *J Mater Sci Mater Electron* 27(1):146–153
102. Kumara N et al (2015) Efficiency enhancement of Ixora floral dye sensitized solar cell by diminishing the pigments interactions. *Sol Energy* 117:36–45
103. Chang H et al (2013) Characterization of natural dye extracted from wormwood and purple cabbage for dye-sensitized solar cells. *Int J Photoenergy*
104. Koli P (2014) Photogalvanic cells: comparative study of various synthetic dyes and natural photo sensitizers present in spinach extract. *Rsc Adv* 4(86):46194–46202
105. Lim A et al (2016) Co-dominant effect of selected natural dye sensitizers in DSSC performance. *Spectrochim Acta Part A Mol Biomol Spectroscopy* 167:26–31
106. Chang H, Lai XR (2016) Fabrication of natural sensitizer extracted from mixture of purple cabbage, roselle, wormwood and seaweed with high conversion efficiency for DSSC. *J Nanosci Nanotechnol* 16(2):2072–2075
107. Kumara NTRN et al (2013) Layered co-sensitization for enhancement of conversion efficiency of natural dye sensitized solar cells. *J Alloy Compd* 581:186–191
108. Bidikoudi M et al (2015) Solidification of ionic liquid redox electrolytes using agarose biopolymer for highly performing dye-sensitized solar cells. *Electrochim Acta* 179:228–236
109. Adel R et al (2015) Effect of polymer electrolyte on the performance of natural dye sensitized solar cells. *Superlattices Microstruct* 86:62–67
110. Thambidurai M et al (2011) Dye-sensitized ZnO nanorod based photoelectrochemical solar cells with natural dyes extracted from Ixora coccinea, Mulberry and Beetroot. *J Mater Sci Mater Electron* 22(11):1662–1666

111. Thambidurai M et al (2014) Rosa centifolia sensitized ZnO nanorods for photoelectrochemical solar cell applications. Sol Energy 106:143–150
112. Thankappan A et al (2015) Highly efficient betanin dye based ZnO and ZnO/Au Schottky barrier solar cell. Thin Solid Films 583:102–107
113. Furukawa S et al (2009) Characteristics of dye-sensitized solar cells using natural dye. Thin Solid Films 518(2):526–529
114. Wongcharee K, Meeyoo V, Chavadej S (2007) Dye-sensitized solar cell using natural dyes extracted from *rosella* and *blue pea* flowers. Sol Energy Mater Sol Cells 91(7):566–571
115. Luo PH et al (2009) From salmon pink to blue natural sensitizers for solar cells: *Canna indica* L., *Salvia splendens*, *cowberry* and *Solanum nigrum* L. Spectrochim Acta Part A Mol Biomol Spectro 74(4):936–942
116. Fernando J, Senadeera GKR (2008) Natural anthocyanins as photosensitizers for dye-sensitized solar devices. Curr Sci 95(5):663–666
117. Hao SC et al (2006) Natural dyes as photosensitizers for dye-sensitized solar cell. Sol Energy 80(2):209–214
118. Jin EM et al (2010) Photosensitization of nanoporous TiO<sub>2</sub> films with natural dye. Phys Scripta T139
119. Calogero G, Di Marco G (2008) Red Sicilian orange and purple eggplant fruits as natural sensitizers for dye-sensitized solar cells. Sol Energy Mater Sol Cells 92(11):1341–1346
120. Polo AS, Murakami Iha NY (2006) Blue sensitizers for solar cells: natural dyes from Calafate and Jaboticaba. Sol Energy Mater Sol Cells 90(13):1936–1944
121. Zhou H et al (2011) Dye-sensitized solar cells using 20 natural dyes as sensitizers. J Photochem Photobiol, A 219(2–3):188–194
122. Calogero G et al (2012) Anthocyanins and betalains as light-harvesting pigments for dye-sensitized solar cells. Sol Energy 86(5):1563–1575
123. Garcia CG, Polo AS, Murakami Iha NY (2003) Fruit extracts and ruthenium polypyridinic dyes for sensitization of TiO<sub>2</sub> in photoelectrochemical solar cells. J Photochem Photobiol, A 160(1–2):87–91
124. Hao S et al (2006) Natural dyes as photosensitizers for dye-sensitized solar cell. Sol Energy 80(2):209–214
125. Ali RAM, Nayan N (2010) Fabrication and analysis of dye-sensitized solar cell using natural dye extracted from dragon fruit. Int J Integr Eng 2:55–62
126. Boyo AO et al (2012) Bitter leaf (*Vernonia amygdalin*) for dye sensitized solar cell. Trends Appl Sci Res 7(7):558–564
127. Dumbravă A et al (2008) Dye-sensitized solar cells based on nanocrystalline TiO<sub>2</sub> and natural pigments. J Optoelectron Adv Mater 10(11):2996–3002
128. Asuloju KA, Shitta MB, Justu S (2011) Effect of extracting solvents on the stability and performances of dye-sensitized solar cell prepared using extract from *Lawsonia inermis*. Fundam J Mod Phys 1(2):261–268
129. Shanmugam V et al (2013) Performance of dye-sensitized solar cells fabricated with extracts from fruits of ivy gourd and flowers of red frangipani as sensitizers. Spectrochim Acta Part A Mol Biomol Spectrosc 104:35–40
130. Hemalatha KV et al (2012) Performance of *Kerria japonica* and *Rosa chinensis* flower dyes as sensitizers for dye-sensitized solar cells. Spectrochim Acta Part A Mol Biomol Spectrosc 96:305–309
131. Senthil TS et al (2011) Natural dye (cyanidin 3-O-glucoside) sensitized nanocrystalline TiO<sub>2</sub> solar cell fabricated using liquid electrolyte/quasi-solid-state polymer electrolyte. Renew Energy 36(9):2484–2488
132. Hamadani M et al (2014) Uses of new natural dye photosensitizers in fabrication of high potential dye-sensitized solar cells (DSSCs). Mater Sci Semicond Process 27:733–739
133. Torchani A et al (2015) Sensitized solar cells based on natural dyes. Curr Appl Phys 15(3):307–312
134. Maurya IC, Srivastava P, Bahadur L (2016) Dye-sensitized solar cell using extract from petals of male flowers *Luffa cylindrica* L. as a natural sensitizer. Opt Mater 52:150–156

135. Phinjaturus K et al (2016) Dye-sensitized solar cells based on purple corn sensitizers. *Appl Surf Sci* 380:101–107
136. Ramamoorthy R et al (2016) Betalain and anthocyanin dye-sensitized solar cells. *J Appl Electrochem* 46(9):929–941
137. Zhang D et al (2008) Betalain pigments for dye-sensitized solar cells. *J Photochem Photobiol A Chem* 195(1):72–80
138. Calogero G et al (2010) Efficient dye-sensitized solar cells using red turnip and purple wild sicilian prickly pear fruits. *Int J Mol Sci* 11(1):254–267
139. Hernandez-Martinez AR et al (2011) New dye-sensitized solar cells obtained from extracted bracts of bougainvillea glabra and spectabilis betalain pigments by different purification processes. *Int J Mol Sci* 12(9):5565–5576
140. Chang H, Lo YJ (2010) Pomegranate leaves and mulberry fruit as natural sensitizers for dye-sensitized solar cells. *Sol Energy* 84(10):1833–1837
141. Chang H et al (2010) Dye-sensitized solar cell using natural dyes extracted from spinach and ipomoea. *J Alloy Compd* 495(2):606–610
142. Hernández-Martínez AR et al (2012) Natural pigment-based dye-sensitized solar cells. *J Appl Res Technol* 10(1):38–47
143. Kumara GRA et al (2006) Shiso leaf pigments for dye-sensitized solid-state solar cell. *Sol Energy Mater Sol Cells* 90(9):1220–1226
144. Lai WH et al (2008) Commercial and natural dyes as photosensitizers for a water-based dye-sensitized solar cell loaded with gold nanoparticles. *J Photochem Photobiol, A* 195(2–3):307–313
145. Taya SA et al (2013) Dye-sensitized solar cells using fresh and dried natural dyes. *Int J Mater Sci Applications* 2(2):37–42
146. Calogero G et al (2014) Brown seaweed pigment as a dye source for photoelectrochemical solar cells. *Spectrochim Acta Part A Mol Biomol Spectrosc* 117:702–706
147. Gomez-Ortiz NM et al (2010) Dye-sensitized solar cells with natural dyes extracted from achiotse seeds. *Sol Energy Mater Sol Cells* 94(1):40–44
148. Zhang D et al (2008) Betalain pigments for dye-sensitized solar cells. *J Photochem Photobiol, A* 195(1):72–80
149. Narayan MR (2012) Review: dye sensitized solar cells based on natural photosensitizers. *Renew Sustain Energy Rev* 16(1):208–215
150. Ludin NA et al (2014) Review on the development of natural dye photosensitizer for dye-sensitized solar cells. *Renew Sustain Energy Rev* 31:386–396
151. Hug H et al (2014) Biophotovoltaics: natural pigments in dye-sensitized solar cells. *Appl Energy* 115:216–225
152. Al-Alwani MAM et al (2016) Dye-sensitised solar cells: Development, structure, operation principles, electron kinetics, characterisation, synthesis materials and natural photosensitisers. *Renew Sustain Energy Rev* 65:183–213
153. Escobar MAM, Jaramillo F (2015) Natural dyes extraction, stability and application to dye-sensitized solar cells. *J Renew Mater* 3(4):281–291

Nanoenergy

Nanotechnology Applied for Energy Production

Souza, F.L.; Leite, E.R. (Eds.)

2018, XII, 330 p. 74 illus., 37 illus. in color., Hardcover

ISBN: 978-3-319-62799-1